JOURNAL OF CATALYSIS 157, 461–471 (1995)

Selectivity in the High-Temperature Hydrogenation of Acetone with Silica-Supported Nickel and Cobalt Catalysts

L. M. Gandia,[1] A. Diaz, and M. Montes

Grupo de Ingeniería Química, Departamento de Química Aplicada, Facultad de Química, Universidad del País Vasco, Apdo. 1072, 20080 San Sebastián, Spain

Received March 30, 1994; revised May 10, 1995; accepted July 28, 1995

In this work, both the physicochemical properties and the selectivity in the acetone hydrogenation for a series of silica-supported nickel and cobalt catalyst were studied. The influence of several preparative aspects, such as the source of the silica support, its sodium content, the calcination temperature and the H_2 reduction temperature of the precursors on the metallic dispersions were investigated. The hydrogenation of acetone was carried out at experimental conditions similar to those necessary for a chemical heat pump application (200°C and high overall acetone conversions). Very high selectivities to 2-propanol are required at these severe and unusual conditions. An excellent performance was found for one of the nickel on silica catalysts which gives selectivities to 2-propanol higher than 99% at 200°C for acetone overall conversions up to 35%. It has been found that the selectivity to this product can be improved by neutralizing the acidic functions of the catalyst. When the sodium content of a poorly alkaline silica is increased, its selectivity to 2-propanol increases due to the suppression of the diisopropyl ether formation. However, an adequate balance between sites is needed since an excessive amount of sodium increases the selectivity to methane. Higher selectivities to 2-propanol were found with Ni compared to Co catalysts due to the formation of methane in significant amounts with Co. The selectivity to 2-propanol decreases as both hydrogenation temperature and acetone feed contents increase, increasing in this way the selectivity to the hydrocracking products. © 1995 Academic Press, Inc.

INTRODUCTION

Catalytic hydrogenations of acetone vapour at temperatures in the 60–180°C range have received considerable attention, but relatively few studies of high equilibrium limited conversions have been reported for higher temperatures in the range 180–220°C. Generally, milder experimental conditions have been selected, giving rise to very good (100%) selectivities to 2-propanol when supported transition metals have been used as catalysts. That is the case, for example, of kieselghur-supported Cu, Pt, Pd, and Rh at 150°C (1, 2), silica-supported Pd and Au in the 150–220°C range (3), Pt on alumina in the range 30 to 90°C (4), and Pt on SiO_2, γ-Al_2O_3, and TiO_2 in the 30–60°C range (5). In those works, acetone conversions lower than 10% were achieved. Cunningham and Al-Sayyed (6) used a Pt on TiO_2 catalyst at 60°C and acetone overall conversions up to 75%. These authors reported selectivities to 2-propanol higher than 98%, the main by-products being low molecular weight (C_1–C_4) hydrocarbons. On the other hand, when unsupported Pt, Ni, Fe, and W have been used as catalysts remarkable selectivities to propane were reported (5, 7, 8), whereas Pd, Au (8), and Cu (9, 10) did not produce propane. As Sen and Vannice (5) pointed out, these differences in selectivity can be explained in terms of the structure-sensitive character of the propane formation through acetone C=O double bond hydrogenolysis.

The hydrogenation of acetone at high temperatures (190–210°C) and conversion (near the chemical equilibrium) is interesting because this reaction can be used in a chemical heat pump for waste heat recovery and upgrading (11). Exceptionally high selectivities to 2-propanol are required for this application. On the other hand, the high temperature reaction between acetone and hydrogen is also of interest since methyl isobutyl ketone (MIBK) can be obtained in a single step and at low pressure, thus reducing the complexity of the commercial processes now available for the manufacture of this valuable chemical.

Previous works (12–15) have shown that both catalyst nature and H_2 reduction pretreatment temperature can have an interesting effect on the selectivity of this reaction. From these works it seems that a correlation exists between the activity for MIBK formation and conditions which lead to a significant presence of metal–support interaction compounds.

In this work, the results obtained in the hydrogenation of acetone in the 180–220°C range with silica-supported nickel and cobalt catalysts are reported. Emphasis has been made on selectivity under these severe conditions. The

[1] Present address: Departamento de Química, Universidad Pública de Navarra, Campus de Arrosadía, 31006 Pamplona, Spain.

0021-9517/95 $12.00

effect of hydrogen reduction temperature for both nickel and cobalt on silica catalysts and that of the sodium content of the support, calcination temperature, feed stream composition, and hydrogenation temperature have been considered. The catalytic behaviour of unsupported nickel and cobalt is also reported.

EXPERIMENTAL

Catalysts

Two families of nickel and cobalt catalysts have been used. In one of them, a silica from Akzo Chemie (F7) was employed, in the other, a silica from Kali Chemie (AF 125) was selected as support. These two silicas will be referred to as SiA and SiK, respectively. All the catalysts were prepared by the incipient wetness technique. Thus, the required amount of an aqueous solution of $Ni(NO_3)_2$ $6H_2O$ or $Co(NO_3)_2$ $6H_2O$ (both Merck, analytical reagent grade) was slowly added to the supports (100–200 μm size fraction) to give solids with a metallic content of between 9 and 15 wt.%. After impregnation, samples were dried overnight at 120°C and then calcined in an air stream (80 ml min^{-1} g_{cat}^{-1}) for 16 h at 500°C. These precursors will be referred to as (SiA–Ni) and (SiA–Co) when the support is SiA and (SiK–Ni) and (SiK–Co) when the metals are supported on SiK. These two silicas have a different sodium content, this being 0.05 wt.% for SiA and 0.2 wt.% for SiK. In order to study the influence of the sodium content on the catalytic properties, a series of samples was prepared by adding increasing amounts of sodium to the support with the lower original sodium content. Thus, three samples of silica from Akzo Chemie were impregnated with aqueous solutions of $NaNO_3$ (Panreac P.A.) so that the sodium content reached 0.1, 0.5, and 1 wt.%, respectively. These samples were dried and calcined in the same way as described above and then impregnated with $Ni(NO_3)_2$ aqueous solutions, dried, and calcined again to give the (SiA–Ni) 0.1%Na, (SiA–Ni) 0.5%Na, and (SiA–Ni) 1%Na precursors. The effect of an additional calcination treatment of the (SiK–Ni) sample for 16 h at 600 or 800°C was also considered, giving rise to the (SiK–Ni) c600 and (SiK–Ni) c800 precursors, respectively. Prior to nickel surface area and catalytic activity measurements, precursors were H_2-reduced (150 cm^3 min^{-1}) at 300 or 500°C. The final catalysts thus resulting will be referred to as their precursors followed by the corresponding reduction temperature (°C) (e.g., (SiK–Ni) 300 is the catalyst that results after H_2 reduction at 300°C of the SiK-supported nickel precursor, and (SiA–Co) 500 is the catalyst that results after H_2 reduction at 500°C of the SiA-supported cobalt precursor). Before exposing the reduced samples to air for X-ray diffraction or transmission electron microscopy measurements, they were passivated at room temperature in an Ar stream (150 cm^3 min^{-1}) containing 100 ppm O_2 for 1.5 h.

Unsupported Ni and Co catalysts were prepared by H_2 reduction (12 h) at 500°C of NiO and Co_3O_4 powders obtained by decomposition in air of the respective nitrates (Merck).

Physicochemical Characterization

Physicochemical characterization included metallic content measurement, nitrogen adsorption, temperature programmed reduction (TPR), X-ray diffraction (XRD), metallic surface area and extent of reduction determinations, and transmission electron microscopy (TEM) observations. Although the experimental procedures have been previously described elsewhere (13, 14), it is convenient to give more details on some of these techniques.

X-Ray Diffraction (XRD)

XRD patterns were obtained and used to estimate the mean metallic crystallite diameters from application of the Scherrer equation (16). XRD line broadening (XRDLB) measurements were carried out with the precursors in order to obtain the average NiO and Co_3O_4 crystallite size resulting after the calcination step using the NiO(200) and Co_3O_4(311) peaks, respectively. In order to obtain the metallic crystallite size for both supported nickel and cobalt, XRDLB measurements were carried out with the reduced and passivated samples, using the Ni(111) and Co(111) peaks, respectively. However, diffraction peaks of metallic cobalt were too weak to make an accurate calculation. Coenen (17) proposed a different and indirect method to calculate the metal particle size, namely, XRDLB measurements carried out over the reduced, passivated, and carefully reoxidized samples. In this work XRDLB measurements of the silica-supported cobalt catalysts were carried out after reoxidation in air of the reduced and passivated samples for 1 h at 500°C. In this case, sizes for the Co_3O_4 phase were obtained, these being finally converted to those corresponding to metallic Co, taking into account the change in the crystalline parameters.

Metallic Surface Area and Extent of Reduction

The Ni surface areas (S_{Ni}) were measured by hydrogen chemisorption with a Micromeritics Pulse Chemisorb 2700. Nickel surface areas were calculated assuming a stoichiometry of one hydrogen molecule adsorbed per two surface nickel atoms, and an area of 6.33 $Å^2$ by each exposed nickel atom (18). The available flow technique was not satisfactory for the cobalt surface area measurement due to the highly reversible character of the hydrogen chemisorption over cobalt (19, 20). The extent of reduction of both nickel and cobalt was measured by means of the

TABLE 1

Metallic Content and Characterization of the Catalysts by Nitrogen Adsorption

Sample	Metal (wt.%)	S_{BET} ($m^2 g_{cat}^{-1}$)	V_p ($cm^3 g_{cat}^{-1}$)	d_p (nm)
SiO_2 Akzo		281	1.57	25
SiO_2 Kali		294	0.78	8.6
(SiA–Ni)	10.0	227	1.29	24
(SiA–Co)	8.6	225	1.28	25
(SiK–Ni)	15.3	233	0.59	8.8
(SiK–Co)	12.8	238	0.62	8.7
(SiA–Ni) 0.1%Na	11.0	232	1.26	24
(SiA–Ni) 0.5%Na	10.0	203	1.27	22
(SiA–Ni) 1%Na	10.7	176	1.16	21
(SiK–Ni) c600	15.4	239	0.60	8.8
(SiK–Ni) c800	14.6	252	0.63	8.8

oxygen uptake in the reoxidation of Ni to NiO at 430°C (21) and that of Co to Co_3O_4 at 400°C (20).

Nickel particle diameters, d_{H_2} (defined as the cube root of the volume) were derived from the metallic surface area and extent of reduction data by assuming that that metallic particles are spherical and wholly exposed to chemisorption and that the unreduced nickel phase is separated from the reduced particles (18, 22, 23).

Acetone Hydrogenation

Acetone hydrogenation reactions were carried out at atmospheric pressure in a fixed-bed reactor that has been described elsewhere (13, 14). Prior to reaction, samples were subjected to a hydrogen (150 ml min^{-1}) reduction treatment for 12 h at 300 or 500°C and then cooled in H_2 to the reaction temperature. Hydrogenation reactions were typically carried out at 200°C with an acetone feed stream composition of 10 mol%, but 180 and 220°C as well as acetone feed stream compositions between 6 and 20 mol% were also used with the (SiA–Ni) precursor. Experiments were carried out at different W/F_{A_0} to evaluate the overall acetone conversions and selectivities for the different reaction products. Reaction rates were measured in differential reactor conditions and selectivities were defined as the molar fraction of the reacted acetone which was converted into a given product.

RESULTS

Nitrogen Adsorption

Table 1 shows the specific surface areas, S_{BET}, and total pore volumes, V_p, of the different samples. The mean pore diameter, d_p, and the metallic content are also included. As can be seen, both silicas have very similar specific surface areas. However, SiA has significant higher pore volume and mean pore diameter. These differences between supports are maintained after catalyst preparation, irrespective of whether the metallic precursor is nickel or cobalt. A loss of specific surface area and pore volume with respect to the supports is observed after the metallic precursor introduction. The preimpregnation of SiA with sodium causes an additional loss of specific surface area and pore volume in the catalyst. No change is found in the textural parameters when (SiK–Ni) is additionally calcined at 600 or 800°C.

TPR

In Figs. 1 and 2, the respective TPR profiles of the SiA- and SiK-supported catalysts are presented. The weight loss associated with the supports is very low. The total weight losses recorded with the catalysts agree reasonably well (within 5% error) with the theoretical weight losses calculated for the reductions of NiO to Ni and Co_3O_4 to Co. A single peak is found at 355°C in the (SiA–Ni) sample TPR curve. This peak is displaced to progressively higher temperatures when the silica has been previously impregnated with increasing amounts of sodium. A new reduction process appears between 450 and 550°C for the (SiA–Ni) 0.5%Na sample and between 600 and 700°C for the (SiA–Ni) 1%Na sample. In the (SiK–Ni) TPR curve two broad peaks at 360 and 530°C are found respectively. When this sample is additionally calcined at 600 or 800°C, distinction between the two peaks is difficult and reduction temperatures are displaced to higher values. The TPR curves of the silica-supported cobalt samples show two peaks in the ranges 250–300°C and 300–500°C, respectively.

Hydrogen Chemisorption and Extent of Reduction

The measured nickel surface areas, S_{Ni}, have been included in Table 2. As can be seen, higher nickel surface areas are obtained for reduction at 300 or 500°C when the

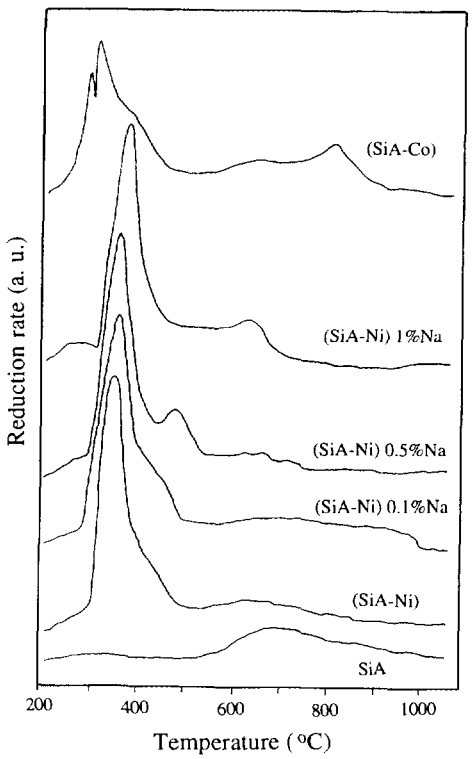

FIG. 1. TPR profiles of the catalysts supported on SiA.

support is SiK. The additional calcination treatment of the (SiK–Ni) sample at 600 or 800°C gives a progressive loss of nickel surface area. The impregnation of the SiA with sodium prior to nickel introduction has little effect on the nickel surface area. All samples gave 100% reduction except (SiK–Ni) c800 and the (SiA–Co) and (SiK–Co) catalysts reduced at 300°C, which showed reduction extents of 0.8, 0.75, and 0.95, respectively.

Mean Particle Diameter

Table 2 presents the mean particle diameters, d_{H_2}, for the nickel samples obtained from the respective metallic surface areas. This table also includes the Ni particle diameter, d_{TEM}, obtained from the respective TEM observations made for three reduced and passivated samples. As can be seen, relatively good agreement has been obtained between H_2 chemisorption and TEM measurements for both (SiK–Ni) 500 and (SiA–Ni) 500 catalysts. On the other hand, the diameter obtained by H_2 chemisorption is 3 times higher than that from TEM for the 300°C reduced (SiK–Ni) c800 catalyst. As shown in Table 2, considerably higher Ni particle diameters were found for the SiA-supported catalysts than for the SiK–supported ones. The preimpregnation of SiA with sodium has little effect on the nickel particle diameter derived from H_2 chemisorption results. On the other hand, whereas a great increase of the nickel particle diameter was found by means of H_2 chemisorption for the (SiK–Ni) catalysts additionally calcined at 600 and 800°C and reduced at 300°C, TEM measurements did not indicate any sintering.

Table 2 also shows the sizes obtained by XRDLB and TEM measurements for the NiO and Co_3O_4 phases in the precursors, for the nickel metallic phase in the reduced and passivated catalysts, and for the metallic Co phase calculated with the passivated and reoxidized sample according to Coenen's method (15). XRDLB measurements were easily made with the reduced and passivated nickel catalysts XRD patterns, which show very well-defined metallic Ni peaks, whereas NiO from the passivation layer is not found. Nevertheless, very weak metallic Co peaks were found with the reduced and passivated cobalt catalysts, it being impossible to make accurate line broadening measurements. XRDLB measurements for cobalt according to the Coenen's method have been performed with the passivated samples reoxidized for 1 h at 500°C. These conditions give complete reoxidation of the metallic Co to Co_3O_4. When reoxidation was carried out for 3 h at 300°C, small diffraction peaks from the remaining metallic phases were still present in the XRD patterns. According to the XRDLB results shown in Table 2, higher dispersions are obtained when nickel is supported on SiK than on SiA. In the case of cobalt, little difference in the precursor size is

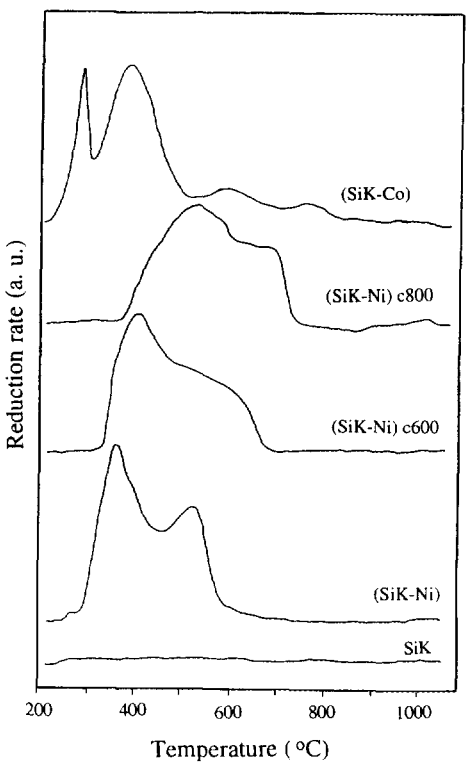

FIG. 2. TPR profiles of the catalysts supported on SiK.

TABLE 2

Nickel Surface Area and Mean Particle Diameters[a] Obtained by XRDLB, TEM, and H_2 Chemisorption

Sample	S_{Ni} ($m^2 g_{Ni}^{-1}$)	Size of the oxide precursors[a]		Metallic Ni particle size[a]			Metallic Co particle size[a]
		XRDLB	TEM[b]	d_{H_2}	XRDLB[c]	TEM[c,d]	XRDLB[e]
(SiA–Ni) 300	11.0	22.6	—	49	18.5	—	—
(SiA–Ni) 500	13.3	22.6	—	41	23.9	37	—
(SiA–Co) 300	—	15.5	—	—	—	—	17.7
(SiA–Co) 500	—	15.5	—	—	—	—	17.7
(SiK–Ni) 300	33.9	11.9	14.3	16	11.5	—	—
(SiK–Ni) 500	39.4	11.9	14.3	14	12.2	18.6	—
(SiK–Co) 300	13.3	—	—	—	—	—	11.3
(SiK–Co) 500	13.3	—	—	—	—	—	11.3
(SiA–Ni) 0.1%Na[f]	9.4	17.8	—	58	16.5	—	—
(SiA–Ni) 0.5%Na[f]	10.5	13.9	—	52	12.6	—	—
(SiA–Ni) 1%Na[f]	12.4	14.8	—	44	14.7	—	—
(SiK–Ni) c600[f]	16.4	12.1	—	33	9.8	—	—
(SiK–Ni) c800[f]	10.2	11.8	14.5	42	9.8	13.8	—

[a] Diameters in nm.
[b] Volume-averaged values.
[c] Diameters obtained with the reduced and passivated samples.
[d] Surface-averaged values.
[e] Diameters obtained according to Coenen's method (15).
[f] This sample was reduced in hydrogen at 300°C.

obtained as a function of the source of silica. The preimpregnation of SiA with increasing amounts of sodium clearly decreases the size of NiO crystallites in the precursor. On the other hand, when the (SiK–Ni) precursor is additionally calcined at 600 or 800°C, sintering of NiO crystallites is not found by XRD. It is also shown that very little change in crystallite size is produced in all cases when precursors are H_2 reduced to give the final catalysts. A moderate agreement is obtained between XRDLB and TEM measurements for both the precursors and the reduced and passivated catalysts supported on SiK. When the support was SiA, significant changes were found in the TEM observations of (SiA–Ni) from the precursor state to the reduced and passivated sample. Thus TEM micrographs of the (SiA–Ni) precursor showed surprisingly large particles, approximately cubic in shape, in the range 100 to 200 nm. The very low contrast of NiO over silica made a more detailed study difficult, but from some high magnification observations the possibility that these particles were aggregates of smaller ones in the 25–40 nm range cannot be discarded. It is noticeable that XRDLB measurements give a value of 22.6 nm for the mean NiO crystallite diameter in the (SiA–Ni) precursor. The large particles are not observed in the TEM micrographs of the reduced and passivated (SiA–Ni) 500 catalyst. In this case, good agreement between TEM and H_2 chemisorption was obtained (see Table 2), whereas XRDLB gave once again a lower Ni mean crystallite diameter (23.9 nm) as compared to TEM results (37 nm).

Activity and Selectivity in the Acetone Hydrogenation

Both silicas were inactive for the acetone conversion after hydrogen treatment at 300 or 500°C. With the silica-supported nickel and cobalt catalysts, 2-propanol (2P) was the main reaction product. A cracking fraction (C), mainly formed by methane and in lower proportion by propane, was routinely found. Diisopropyl ether (DIPE) with the silica-supported nickel, and methyl isobutyl ketone (MIBK) with the silica-supported cobalt catalysts, were also found as by-products. Table 3 shows the activity of the samples expressed as rates of formation of the different reaction products. Experiments were carried out at 200°C with a feed stream composed by 10 mol% acetone in hydrogen. Reaction rates were obtained at 10% acetone overall conversion. As cobalt surface areas were not available, only turnover numbers (TON) for 2-propanol formation of the nickel catalysts have been calculated on the basis of the number of exposed nickel atoms estimated from nickel surface area measurements. These results have been included in Table 3. As can be seen, only minor differences in TON were observed, but higher specific activities were obtained when the nickel catalysts are reduced at 300°C than at 500°C. Higher TON values were also obtained

TABLE 3

Catalytic Activity in the Acetone Hydrogenation at 200°C, with 10 Mol% Acetone in Feed[a]

Sample	r_{2P}[b]	r_C[b]	r_{DIPE}[b]	r_{MIBK}[b]	TON[c]
(SiA–Ni) 300	11.5	0.090	0.012	—	11
(SiA–Ni) 500	8.1	0.072	0.008	—	6.4
(SiA–Co) 300	8.6	0.195	—	—	—
(SiA–Co) 500	6.1	0.171	—	0.012	—
(SiK–Ni) 300	17.7	0.180	—	—	5.5
(SiK–Ni) 500	14.0	0.114	—	—	3.8
(SiK–Co) 300	11.2	0.570	—	—	—
(SiK–Co) 500	8.6	0.390	—	0.009	—
(SiA–Ni) 0.1%Na[d]	14.2	0.084	—	—	16
(SiA–Ni) 0.5%Na[d]	10.0	0.120	—	—	10
(SiA–Ni) 1%Na[d]	9.4	0.114	—	—	8
(SiK–Ni) c600[d]	15.3	0.165	—	—	9.9
(SiK–Ni) c800[d]	9.1	0.129	—	—	9.4

[a] (2P) 2-propanol, (C) cracking fraction (assumed to be methane), (DIPE) diisopropyl ether, (MIBK) methyl isobutyl ketone.

[b] Rates in (mol of product formed h^{-1} g^{-1}_{metal}) calculated at 10% overall acetone conversion.

[c] Turnover numbers for 2-propanol formation (s^{-1}).

[d] This sample has been reduced in hydrogen at 300°C.

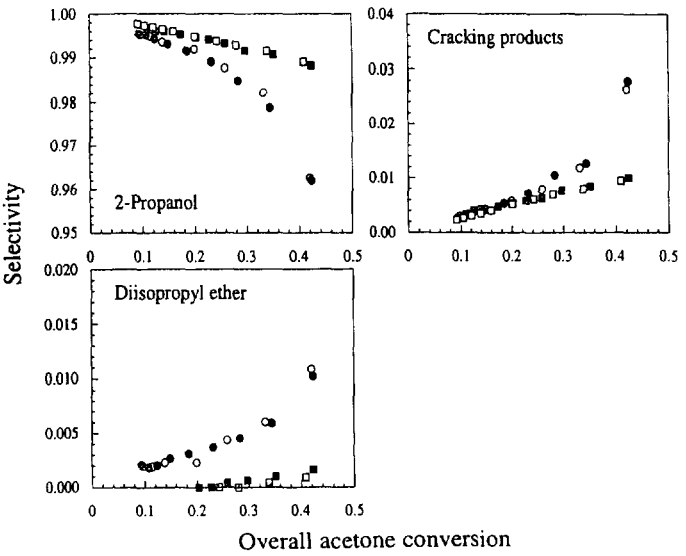

FIG. 3. Selectivities of the (SiA–Ni) 300 (●); (SiA–Ni) 500 (○); (SiK–Ni) 300 (■); and (SiK–Ni) 500 (□) catalysts at 200°C with 10 mol% acetone in the feed.

when nickel was supported on SiA. When the (SiK–Ni) precursor was additionally calcined at 600 or 800°C the specific activity increased and similar values to that of SiA-supported nickel were obtained. The preimpregnation of SiA with a very low amount of sodium (0.1 wt.%) increases the specific activity.

The effect of the acetone hydrogenation temperature was explored with the (SiA–Ni) 500 catalyst in the range 180 to 220°C, and an apparent activation energy of 8.9 kcal mol^{-1} was obtained.

The selectivities to 2-propanol, cracking products, and diisopropyl ether of the (SiA–Ni) and (SiK–Ni) catalysts, both reduced at 300 and 500°C, are shown in Fig. 3. It can be seen that selectivity was not affected by the temperature of reduction of nickel on silica catalysts. Very high selectivities to 2-propanol (>96%) were obtained taking into account the noticeable high temperature of hydrogenation and acetone overall conversions, which was in some experiments close to the equilibrium acetone hydrogenation conversion (43% at 200°C). It is remarkable to note the excellent behaviour of nickel on SiK catalyst, which gave selectivities to 2-propanol higher than 99% for overall acetone conversions of up to 35%. Nickel on SiA showed lower selectivities to 2-propanol, which was mainly due to the relatively high activity of this catalyst for the diisopropyl ether formation.

The effect of preimpregnation of SiA with increasing amounts of sodium on the selectivity of supported nickel is shown in Fig. 4, where the curves for the (SiA–Ni) and (SiK–Ni) catalysts have been included as references. Catalysts were tested after H_2 reduction at 300°C for 12 h. As can be seen, the selectivity to 2-propanol of the (SiA–Ni) catalyst was improved when the sodium content of the support was increased to 0.1 wt.%, giving a selectivity comparable or slightly higher than that of the (SiK–Ni) catalyst. This result is due to a great decrease in the produc-

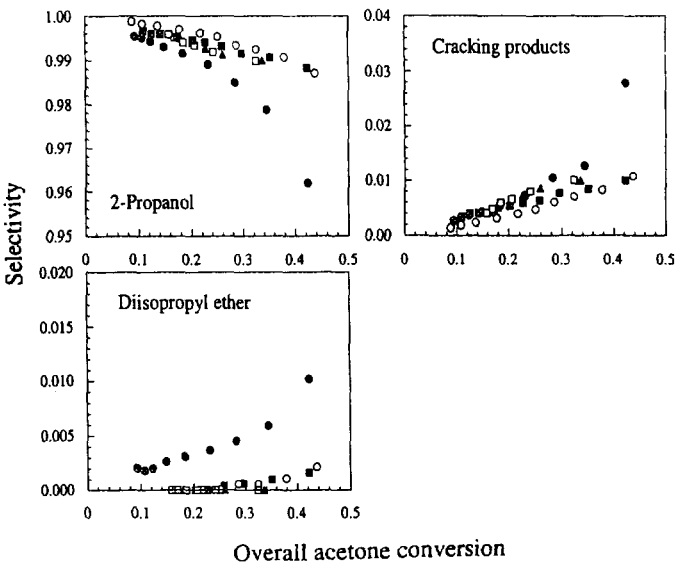

FIG. 4. Selectivities of the (SiA–Ni) (●), (SiK–Ni) (■), (SiA–Ni) 0.1%Na (○), (SiA–Ni) 0.5%Na (▲), and (SiA–Ni) 1%Na (□) catalysts at 200°C with 10 mol% acetone in the feed after H_2 reduction at 300°C.

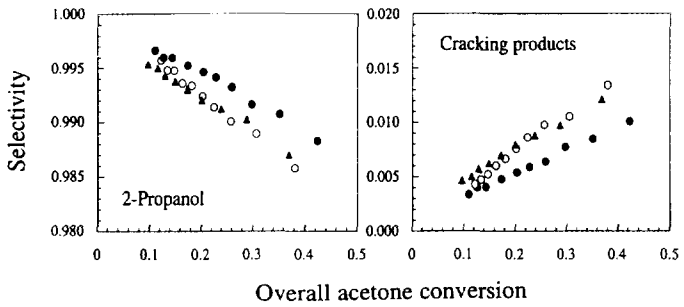

FIG. 5. Selectivities of the (SiK–Ni) (●), (SiK–Ni) c600 (○), and (SiK–Ni) c800 (▲) catalysts at 200°C with 10 mol% acetone in the feed after H_2 reduction at 300°C.

tion of both cracking products and diisopropyl ether. However, for higher sodium contents (0.5 and 1 wt.%), in spite of the complete suppression of the formation of diisopropyl ether, the selectivity to 2-propanol decreased with respect to that of the (SiA–Ni) 0.1%Na, because the activity for the formation of cracking products had increased. The effect of an additional calcination treatment at 600 or 800°C on the selectivity of the (SiK–Ni) catalyst is shown in Fig. 5. Catalysts were tested after H_2 reduction at 300°C for 12 h. As can be seen, little difference was found between (SiK–Ni) c600 and (SiK–Ni) c800 samples, which give lower selectivity to 2-propanol and higher selectivity to cracking products than the (SiK–Ni) catalyst.

The effect of the feed stream acetone composition on the selectivity of the (SiA–Ni) 500 catalysts in the acetone hydrogenation at 200°C is shown in Fig. 6. The selectivity

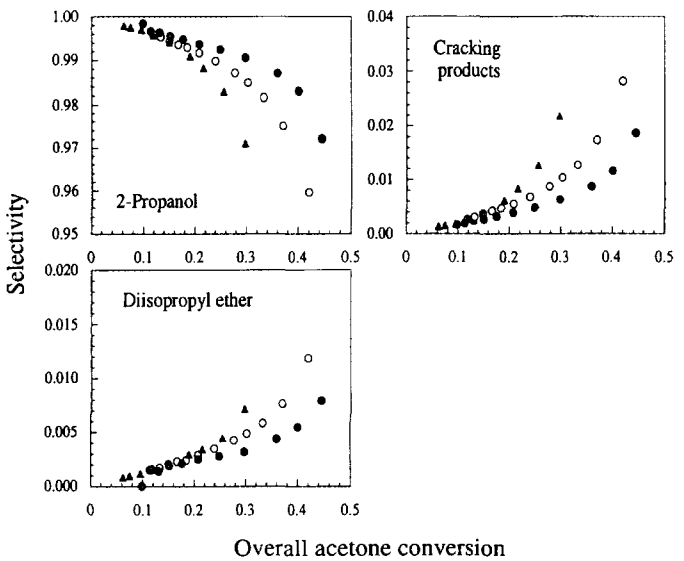

FIG. 6. Effect of the acetone feed stream composition on the selectivity at 200°C of the (SiA–Ni) 500 catalyst; 6 mol% (●), 10 mol% (○), and 20 mol% (▲).

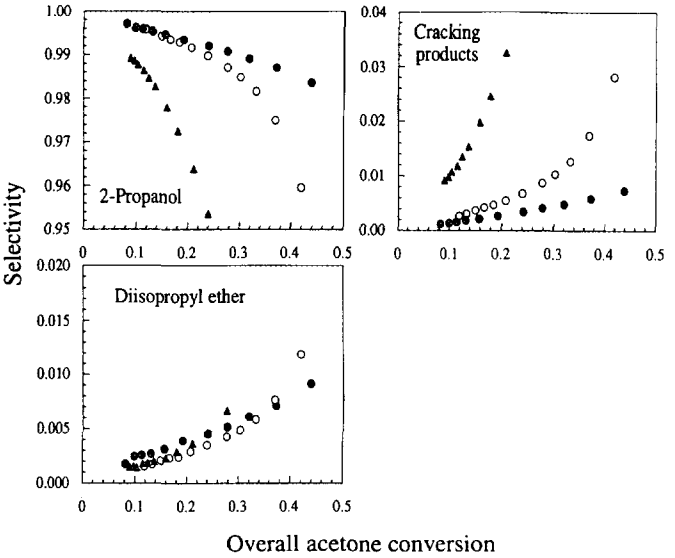

FIG. 7. Effect of the acetone hydrogenation temperature on the selectivity of the (SiA–Ni) 500 catalyst with 10 mol% acetone in the feed, 180°C (●), 200°C (○), and 220°C (▲).

to 2-propanol decreased and that to both cracking products and diisopropyl ether increased as the proportion of acetone in the feed increased from 6 to 20 mol%. This was also the case when the temperature of the acetone hydrogenation was increased from 180 to 220°C, as can be seen in Fig. 7. However, in this case the differences in selectivity promoted by the reaction temperature were mainly due to the formation of cracking products since selectivities to diisopropyl ether showed little change.

The selectivities to 2-propanol, cracking products, and methyl isobutyl ketone of the (SiK–Co) and (SiK–Co) catalysts, both reduced at 300 and 500°C, are shown in Fig. 8. Selectivities to 2-propanol of the (SiA–Ni) 300 and (SiK–Ni) 300 catalysts have been included as references. As can be seen, nickel is more selective to 2-propanol than cobalt. This difference was enhanced when both metals were supported on SiK, and it was mainly due to the relatively high activity of cobalt samples to form cracking products. Diisopropyl ether was not found with the cobalt on silica catalysts; however, MIBK was produced. Selectivity to this product showed little dependence on the acetone overall conversion, and values of 0.1–0.2% for (SiK–Co) 300 and 0.3–0.5% for (SiA–Co) 500 were obtained. Selectivity to MIBK increased as temperature of reduction for both (SiA–Co) and (SiK–Co) was increased from 300 to 500°C. In contrast with nickel, the selectivity of the cobalt on silica catalysts was affected by the temperature of reduction. Hence, whereas the selectivity to 2-propanol of (SiK–Co) increased slightly when the temperature of reduction was increased from 300 to 500°C, that of (SiA–Co) decreased slightly.

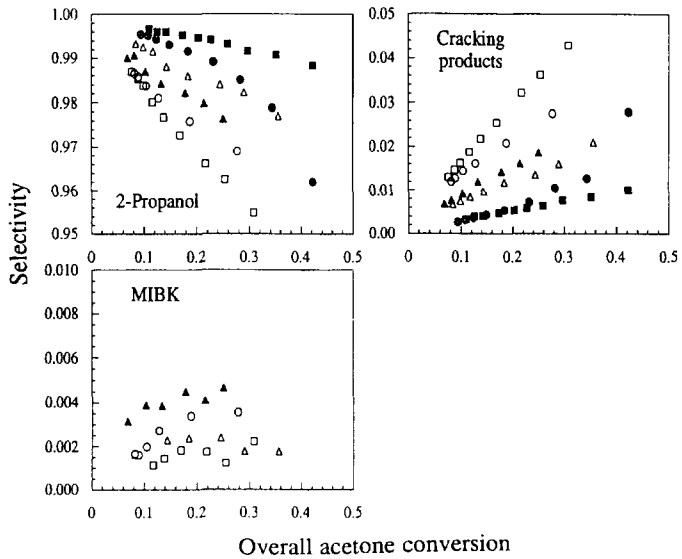

FIG. 8. Selectivities of the (SiA–Ni) 300 (●), (SiK–Ni) 300 (■), (SiA–Co) 300 (△), (SiA–Co) 500 (▲), (SiK–Co) 300 (□), and (SiK–Co) 500 (○) catalysts at 200°C with 10 mol% acetone in the feed.

The catalytic behaviour of unsupported nickel and cobalt after reduction in hydrogen at 500°C was studied. The metallic powders showed very low activity and acetone overall conversions between 1.5 and 2.5% were achieved. Unsupported nickel gave very good selectivity to 2-propanol (>99.5%), methane and propane being the only by-products. In contrast with nickel, unsupported cobalt was remarkably selective to acetone aldol condensation products and selectivities up to 25% to MIBK and 17% to mesityl oxide were obtained.

DISCUSSION

TPR and Extent of Reduction

The TPR results obtained with nickel on SiK catalysts (see Fig. 2) are in agreement with the work of Mile *et al.* (24, 25). Thus, the peaks at 360 and 530°C can be attributed to the reduction of bulk NiO particles and Ni^{2+} ions in interaction with the support, respectively, in the form of a few surface layers of silicate-type compounds. The larger contribution of the high-temperature peak to the overall reduction and the displacement of this peak to higher temperatures shown by the additionally calcined samples at 600 and 800°C would be in agreement with a double effect: (i) an increased fraction of the nickel would form interaction compounds, as suggested by the incomplete extent of reduction found for the (SiK–Ni) c800 sample, and (ii) the NiO surface becames progressively smooth as a consequence of the annihilation of steps, terraces, kinks, etc. that act as nucleation sites for the process of oxide reduction, which becomes more difficult (26).

The displacement to higher temperatures of the TPR peaks found for the Ni catalysts prepared on SiA previously impregnated with sodium (see Fig. 1) can be explained in terms of an increased interaction of NiO with sodium-rich areas of the support, where the formation of poorly reducible mixed oxides of Si^{4+}, Na^{+}, and Ni^{2+} during the preparation of the catalyst is very likely, as suggested by Houalla *et al.* (27). This explanation could also be valid for the higher contribution to the overall reduction of the high-temperature region (400–500°C) found for both Ni and Co on SiK than when they were supported on SiA, which has a lower sodium content.

The TPR profiles of cobalt on silica catalysts show that the reduction process was not completed, even at temperatures up to 600°C. This fact, in conjunction with the incomplete extents of reduction that have been found for cobalt on silica catalysts after reduction at 300°C suggest that some of the cobalt ions are in interaction with the support, probably in the form of poorly reducible silicate-type compounds. Thus, Srinivasan *et al.* found unreduced CoO in cobalt on silica catalysts reduced at 350°C (28). Puskas *et al.* found a remarkable tendency of cobalt to form silicates in Co/SiO_2 systems when the conditions of preparation of the catalysts are favourable to a partial dissolution of the support (29).

Mean Metallic Particle Diameter

There is general agreement that hydrogen chemisorption and TEM are the most suitable techniques for the determination of the supported nickel and cobalt particle diameters, whereas XRDLB generally shows a lack of accuracy for metallic particles in the 5–15 nm range (20, 30). In our work, the agreement between techniques has been influenced by the source of the silica support, as well as by treatments such as additional calcination of the precursor. Thus, a reasonably good agreement was obtained between the three techniques for the (SiK–Ni) 500 catalyst and between XRD and TEM for the (SiK–Ni) precursor (see Table 2). On the other hand, when the support was SiA, good agreement between H_2 chemisorption and TEM was found for the (SiA–Ni) 500 catalyst, but XRDLB measurements gave a notably lower Ni crystallite size (see Table 2). These results can be explained taking into account that XRDLB measurements depend on the crystallite size, TEM permits particles that could be composed of smaller crystallites to be detected and H_2 adsorption give an equivalent particle size depending on the shape used for calculations. Agreement between these techniques can be obtained only when particles are monocrystals with a known and smooth shape.

As shown previously, relatively good agreement between the three techniques has been achieved with the (SiK–Ni) precursor and the (SiK–Ni) 500 catalyst. How-

ever, whereas both XRD and TEM showed that little particle diameter change takes place, when the (SiK–Ni) precursor was additionally calcined at 800°C to give the (SiK–Ni) c800 sample, an important increase in the Ni particle diameter derived from H_2 chemisorption measurements is observed after reduction at 300°C of the (SiK–Ni) c800 precursor (see Table 2). In consequence, the decrease in the Ni surface area for the (SiK–Ni) c600 and (SiK–Ni) c800 samples with respect to (SiK–Ni) is not due to nickel sintering. This decrease could be due to modification of the chemisorptive properties of the reduced metal as a consequence of the previous high-temperature calcination. It is well known that the reversibility of H_2 chemisorption over Ni increases as the metal–support interation increases (19). Therefore, if as a consequence of the high-temperature calcination step the proportion of reversibly chemisorbed hydrogen increases, these molecules would be difficult to detect by a dynamic pulse method (19, 20), as used in this work.

Activity and Selectivity in the High-Temperature Acetone Hydrogenation

Relatively few studies have been reported on the catalytic reaction between acetone and hydrogen in the range 180–220°C and high equilibrium-limited conversions (12–15, 31).

The rates of formation of the different products of reaction have been included in Table 3. As can be seen, rates for all the reaction products decrease proportionally when the temperature of reduction of the (SiA–Ni) and (SiK–Ni) catalysts increases from 300 to 500°C; in consequence, there are no changes in selectivity as a function of the temperature of reduction for the nickel on silica catalysts (see Fig. 3). Differences in selectivity for the nickel catalysts prepared over the two different silicas can be explained in terms of the sodium content of the silica. Higher selectivities to 2-propanol were obtained with nickel supported on SiK (0.2 wt.% Na) compared to nickel supported on SiA (0.05 wt.% Na). This is mainly due to the very low activity of the nickel on SiK catalyst for diisopropyl ether formation (see Fig. 3). The effect of sodium is demonstrated by the fact that when nickel was supported on SiA previously impregnated with sodium, the activity for diisopropyl ether formation decreased and the selectivity to 2-propanol was significantly increased, reaching a maximum for the (SiA–Ni) 0.1%Na catalyst. However, for higher sodium contents (0.5 and 1 wt.%), the selectivity to 2-propanol decreased since the activity to 2-propanol formation decreased, whereas that for the cracking products formation increased slightly (see Fig. 4 and Table 3). Thus an adequate balance is needed between the acid sites of the catalyst and the sodium added to neutralize these sites, to improve the selectivity to 2-propanol. A small number of acid sites, coming from silica or from the interface between reduced Ni and unreduced nickel silicate-type compounds, explains the formation of diisopropyl ether over (SiA–Ni) (32). If little sodium is added, the acid sites can be neutralized and no ether is produced, as over (SiA–Ni) 0.1%Na. However if sodium is added in excess, (SiA–Ni) 0.5%Na and (SiA–Ni) 1%Na, new basic sites are likely to be produced which could be responsible for the increased activity in the formation of cracking products. These results are in agreement with those obtained by Krauss *et al.* (32, and references therein), who studied the conversion of alcohols to ethers in hydrogen with nickel on silica catalysts at temperatures close to those used in this work. As these authors pointed out, the ether formation occurs via a concerted *trans*-elimination mechanism over an acid–base pair site. These sites have their origin in an cooperative effect of the reduced Ni with nickel silicate-type sites resulting in an increased acidity of the catalyst (32).

When the (SiK–Ni) catalyst was additionally calcined at 600 or 800°C nickel sintering was not found by XRDLB and TEM, the main effect being an important decrease in the extent of reduction for the (SiK–Ni) c800 catalyst, which produced little effect on selectivity (see Fig. 5). A decrease in the 2-propanol selectivity was found for these catalysts that was due to a higher decrease in the activity to 2-propanol formation than that to cracking products (see Table 3). These changes can be related to the different effects of the treatments on both reactions, hydrogenation and hydrogenolysis (to cracking products), it being usually accepted that hydrogenolysis is a structure-sensitive reaction (22, 33).

It has been shown that the selectivity to 2-propanol of the (SiA–Ni) 500 catalyst decreases as the hydrogenation temperature increases (see Fig. 7). This effect is due to a larger increase in the rate of formation of the cracking products than that of the others. The increase in acetone cracking activity to methane and CO at increasing acetone adsorption temperatures on a silica-supported nickel catalyst has been previously found by Young and Sheppard (34). According to these authors the decomposition process is favoured thermodynamically at increasing temperatures.

In this work several differences have been found between the catalytic behaviour of nickel and cobalt on silica catalysts.

(i) Lower selectivities to 2-propanol are obtained with Co than with Ni (see Fig. 8). This is mainly due to the higher activity showed by the Co samples to the formation of cracking products. This behaviour could be explained by the apparent higher reactivity of Co towards acetone compared with Ni, as suggested by the IR study made by Blyholder and Shihabi (35). These authors found much

more acetone adsorbed on Co than on Ni at 90°C and in a great variety of forms (coordinated acetone, isopropoxide, and acyl groups).

(ii) Whereas the temperature of reduction had no effect on the selectivity of the Ni on silica catalysts, the 2-propanol selectivity of (SiA–Co) decreased and that of (SiK–Co) slightly increased as the temperature of reduction increased from 300 to 500°C. From the results in Table 3, these differences probably arise from the more important decrease found for (SiK–Co) than for (SiA–Co) in the activity to cracking product formation, whereas activity to 2-propanol formation is affected approximately in a similar way for both catalysts. It is likely that changes associated with a higher H_2 treatment temperature could be related to the reduction of oxidized Co ions associated with cobalt–silica interaction compounds. The contribution to the overall catalytic activity of the oxidized forms of cobalt cannot be discarded (36). However, the contribution of other factors, such as the lower sodium content of SiA, and hence their likely higher acidity, could explain the relatively low decrease in the activity to cracking products found for the (SiA–Co) catalyst, in spite of the increase from 75 to 100% in their extent of reduction when the reduction temperature is increased to 500°C.

(iii) Whereas diisopropyl ether was found in significant amounts only with the nickel on SiA catalysts, methyl isobutyl ketone (MIBK) was found (in very low amounts) only with the silica-supported cobalt catalysts. Unsupported Ni powder was not active for diisopropyl ether and MIBK formation. On the other hand, neither did unsupported cobalt powder give diisopropyl ether but showed good selectivity to MIBK. It is noticeable that when these metals are supported on silica, MIBK was observed only over silica-supported cobalt, as in the case of the unsupported metals. The formation of diisopropyl ether is affected by the support nature. Silica can add active sites for this reaction (over the support itself, or on the metal–support interface), or it can also produce different morphology nickel particles and hence new metallic active sites. The sodium content of the silica was shown to play an important role, but unfortunately it does not allow us to distinguish between the previous hypotheses, because it influences both of them in the same way.

Finally, some information about the reaction scheme of the high-temperature acetone hydrogenation over nickel and cobalt silica-supported catalysts can be extracted from the selectivity versus overall acetone conversion curves obtained in this work. Thus, as a general behaviour (see Figs. 3 to 8), selectivity to 2-propanol goes to 100% and that to cracking products and diisopropyl ether readily go to zero as the overall acetone conversion decreases. On the other hand, as shown in Fig. 8, MIBK selectivity seems to be less affected by the overall acetone conversion. These results could be in agreement with a reaction scheme so that acetone is hydrogenated to 2-propanol on the surface of reduced Ni or Co sites. The alcohol can be dehydrated in series to diisopropyl ether with the aid of the acid sites of the catalyst and also hydrogenolyzed to methane. On the other hand, it is reasonable that MIBK is formed via a route parallel to that of hydrogenation, consisting of acetone autocondensation and dehydration to mesityl oxide and selective hydrogenation of this product over metallic sites to give MIBK. This general scheme is consistent with previous results obtained in the high-temperature reaction of acetone and hydrogen over Ni on magnesia (12), Ni and Co over activated charcoal (13), and alumina and titania (14) and Cu on titania (31).

ACKNOWLEDGMENT

Financial support by the Excelentísima Diputación Foral de Guipúzcoa is gratefully appreciated.

REFERENCES

1. Simoniková, J., Ralková, A., and Kochloefl, K., *J. Catal.* **29,** 412 (1973).
2. Simoniková, J., Hillaire, L., Panek, J., and Kochloefl, K., *Z. Phys. Chem. NF* **83,** 287 (1973).
3. Nakamura, M., and Wise, H., "Proceedings, 6th International Congress on Catalysis, London, 1976" (G. C. Bond, P. B. Wells, and F. C. Tompkins, Eds.), p. 881. The Chemical Society, London, 1977.
4. Rositani, F., Galvagno, S., Poltarzewski, Z., Staiti, P., and Antonucci, P. L., *J. Chem. Tech. Biotechnol.* **35A,** 234 (1985).
5. Sen, B., and Vannice, M. A., *J. Catal.* **113,** 52 (1988).
6. Cunningham, J., and Al-Sayyed, G. H., *Nouv. J. Chim.* **8,** 469 (1984).
7. Farkas, A., and Farkas, L., *J. Am. Chem. Soc.* **61,** 1336 (1939).
8. Stoddart, C. T. H., and Kemball, C., *J. Colloid Sci.* **11,** 532 (1956).
9. Cunningham, J., Al-Sayyed, G. H., Cronin, J. A., Healy, C., and Hirschwald, W., *Appl. Catal.* **25,** 129 (1986).
10. Cunningham, J., McNamara, D., Fierro, J. L. G., and O'Brien, S., *Appl. Catal.* **35,** 381 (1987).
11. Gandía, L. M., and Montes, M., *Int. J. Energy Res.* **16,** 851 (1992).
12. Gandía, L. M., and Montes, M., *Appl. Catal. A General* **101,** L1 (1993).
13. Gandía, L. M., and Montes, M., *J. Mol. Catal.* **94,** 347 (1994).
14. Gandía, L. M., and Montes, M., *J. Catal.* **145,** 276 (1994).
15. Gandía, L. M., and Montes, M., *React. Kinet. Catal. Lett.* **53,** 261 (1994).
16. Klug, H. P., and Alexander, L. E., "X-Ray Diffraction Procedures," p. 618. Wiley, New York, 1974.
17. Coenen, J. W. E., *Appl. Catal.* **75,** 193 (1991).
18. Coenen, J. W. E., and Linsen, B. G., *in* "Physical and Chemical Aspects of Adsorbents and Catalysts" (B. G. Linsen, Ed.), p. 471. Academic Press, New York, 1970.
19. Bartholomew, C. H., *in* "Hydrogen Effects in Catalysis" (Z. Páal and D. G. Menon, Eds.), p. 146. Dekker, New York, 1988.
20. Reuel, R. C., and Bartholomew, C. H., *J. Catal.* **85,** 63 (1984).
21. Bartholomew, C. H., and Farrauto, R. J., *J. Catal.* **45,** 41 (1976).
22. Aguinaga, A., De La Cal, J. C., Asúa, J. M., and Montes, M., *Appl. Catal.* **51,** 1 (1989).
23. Gil, A., Díaz, A., and Montes, M., *J. Chem. Soc. Faraday Trans.* **87,** 791 (1991).
24. Mile, B., Stirling, D., Zammitt, M., Lovell, A., and Webb, M., *J. Catal.* **114,** 217 (1988).

25. Mile, B., Stirling, D., Zammitt, M., Lovell, A., and Webb, M., *J. Mol. Catal.* **62,** 179 (1990).
26. Coenen, J. W. E., *in* "Preparation of Catalysts II" (B. Delmon, P. Grange, P. A. Jacobs, and G. Poncelet, Eds.), p. 89. Elsevier, Amsterdam, 1979.
27. Houalla, M., Delannay, F., and Delmon, B., *in* "Preprints of the 7th Canadian Symposium on Catalysis" (S. E. Wanke and K. Chakrabarty, Eds.), p. 158. Chemical Institute of Canada, Edmonton, 1980.
28. Srinivasan, R., De Angelis, R. J., Rencroft, P. J., Dhere, A. G., and Betley, J., *J. Catal.* **116,** 144 (1989).
29. Puskas, I., Fleisch, T. H., Hall, J. B. Meyers, B. L., and Roginski, R. T., *J. Catal.* **134,** 615 (1992).
30. Mustard, D. G., and Bartholomew, C. H., *J. Catal.* **67,** 196 (1981).
31. Cunningham, J., Hickey, J. N., Brown, N. M. D., and Meenan, B. J., *J. Mater. Chem.* **3,** 743 (1993).
32. Krauss, L. S., Pines, H., and Butt, J. B., *J. Catal.* **128,** 337 (1991).
33. Sinfelt, J. H., *Adv. Catal.* **23,** 91 (1973).
34. Young, R. P., and Sheppard, N., *J. Catal.* **7,** 223 (1967).
35. Blyholder, G., and Shihabi, D., *J. Catal.* **46,** 91 (1977).
36. Ponec, V., *Catal. Today* **12,** 227 (1992).